

Efficiency analysis of the SVPWM control using the simulink electrical library and implemented in the Lucas Nulle practice modules

Franklin Israel Sánchez-Gamboa

Higher Technology Research Department in Electromechanics, Instituto Superior Tecnológico Cotopaxi, Cotopaxi, Ecuador. fisanchezg@istx.edu.ec

Received: February 5th, 2023. Received in revised form: June 29th, 2023. Accepted: July 17th, 2023.

Abstract

The purpose of this research is to analyze the efficiency of an induction motor controller, using space vector pulse width modulation (SVPWM) in open loop. With a constant torque of 1.5 Newton per meter. It is carried out by applying the mathematical model, the formulas for commutation times and space vectors in Simulink taking into account the maximum and minimum values of operation by applying the SVPWM method to generate the trigger signal in the Insulated Gate Bipolar Transistor bridge. (IGBT's), implementing the model in the Lucas Nulle practice module, taking the power data and calculating the efficiency to compare with the mathematical model and validate, resulting that the controller efficiency varies according to the switching speed of the semiconductor block, with the operation of a motor of 0.37kW and 1KW at a speed of 200rpm the efficiency of the controller reaches a value of 72.67% in the physical model that consists of 6 IGBT's of 1 kVA and 69% in the simulated model presenting an error of 5% and a switching speed of the IGBT's of 248.641ms.

Keywords: vector; induction motor; efficiency; pulse width control; simulink.

Análisis de eficiencia del control SVPWM utilizando la librería eléctrica de simulink e implementado en los modulos de prácticas Lucas Nulle

Resumen

Esta investigación tiene como objetivo analizar la eficiencia del controlador de un motor de inducción, mediante modulación de ancho de pulso de vector de espacio (SVPWM) en lazo abierto. Con un torque constante de 1.5 Newton por metro. Se lleva a cabo aplicando el modelo matemático, las fórmulas de tiempos de conmutación y vectores de espacio en Simulink tomando en cuenta los valores máximos y mínimos de operación aplicando el método SVPWM para generar la señal de disparo en el puente de Transistores Bipolares de Puerta Aislada (IGBT's), implementando el modelo en el módulo de prácticas Lucas Nulle tomando los datos de potencia y calculando la eficiencia para comparar con el modelo matemático y validar, resultando que la eficiencia del controlador varía según la velocidad de conmutación del bloque de semiconductores, con la operación de un motor de 0.37kW y 1KW a una velocidad de 200rpm la eficiencia del controlador alcanza un valor de 72.67% en el modelo físico que consta de 6 IGBT's de 1 kVA y 69 % en el modelo simulado presentando un error del 5 % y una velocidad de conmutación de los IGBT's de 248.641ms.

Keywords: vector; motor de inducción; eficiencia; control de ancho de pulso; simulink.

1. Introduction

According to [1] Induction motors are widely used in industrial processes to supply mechanical power and thus perform

tasks that require great effort. In these machines there is difficulty in the implementation of linear control techniques, since the speed at which they rotate and the power they deliver depend on the frequency of the input signal and the supply voltage.

How to cite: Sánchez-Gamboa, F.I., Efficiency analysis of the SVPWM control using the simulink electrical library and implemented in the lucas nulle practice modules. DYNA, 90(227), pp. 66-76, July - September, 2023.

According to [2] Studies show that electric motors by using 60% of industrial electricity are greatest consumer in industrial equipments and have considerable potential for energy efficiency.

According [3] Industry consumes about 40% of the electricity, of which two thirds are used by electric motors. Variable Speed Drives (VSDs), which regulate the speed of motors, can reduce their energy consumption by 50% in many applications, but less than 10% of motors are equipped with such a device.

According [4] The 24-sector SVPWM techniques overcome the drawbacks of PWM and offer great advantages from the point of view of harmonic performances and the easiness in digital implementation. However, the algorithm and digital implementation process are still rather complex.

Therefore, it is proposed to analyze if the SVPWM control technique is more efficient than the conventional PWM control technique with lucas nulle laboratory equipment under load operating conditions.

The analysis is based on the mathematical modeling of the space vector pulse width modulation control using the Simulink electrical library and subsequently implementing the system with Lucas nulle laboratory equipment using a 0.37 and 1 kW triphasic induction motor with a 1.5 N*m load at 200 rpm, 1300 rpm, 3600 rpm operating speeds.

Finally, it is considered that the analysis of the efficiency in the control stage will allow to apply these techniques at an industrial level with knowledge under load operation and will serve as a tool for the industrial community related to the operation of three-phase induction electric motors.

2. Literature review

2.1 Induction motor

Fig. 1 shows an induction motor with a squirrel cage rotor. A three-phase set of voltages has been applied to the stator and a three-phase set of currents flows from it. These currents produce a counterclockwise rotating BS magnetic field. [5]

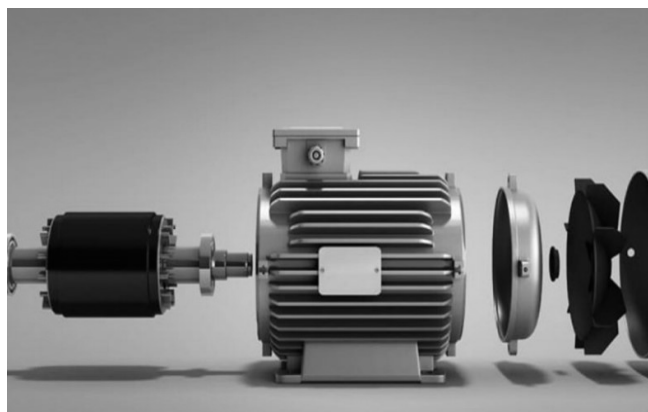


Figure 1. Induction motor.
Source: S. Franklin, 2022

2.2 Frequency inverter

The variable frequency drive as seen in Fig. 2 is the effective solution to improve energy efficiency, reduce energy consumption and carbon dioxide emissions. On this page we will talk about the characteristics, advantages and operation of variable frequency drives.

2.3 Space Vector Pulse Width Modulation (SVPWM)

One of the main characteristics is that the entire triphasic system is represented by a single vector. The SVPWM technique refers to the selection of the switching states of the inverter switches in each existing period by means of times and a determined order. [6]

According [6] there are several applications in which SVPWM modulation presents advantages, for example, in control of three-phase motors, the motor variables can be broken down to have independent control of speed and torque. Also for electric power generation through devices that deliver DC direct voltage, or any application in digital controllers because its implementation becomes simpler than any other PWM modulation.

2.3.1 Switching states in inverters with SVPWM modulation

One In Fig. 2, it is observed that the three-phase inverter has 6 switching devices that will be called switches, the power supply is direct current, the assigned switches S1, S2, S3, S4, S5, S6 of the three-phase inverter they can never be both from the same branch closed. [7]

In state ON or logic 1 because a short circuit occurs in the inverter; that is, while S1 = 1 compulsorily S4 = 0, and so on with the two remaining pairs being their inverse complement. [7]

The switching states are determined only with the upper switches, in this case they are S1, S3 and S5, there are 8 different states with a switching logic that generate sinusoidal triphasic signals, the states are presented in Fig. 5. [7]

The vectors V_0 and V_7 are called null vectors or zero vectors. This occurs when the 3 upper switches are closed or open and there is no voltage, on the contrary, the other vectors are called active vectors and with the Clarke transform, Fig. 3 is presented, which corresponds to the voltage values in each state. [7]

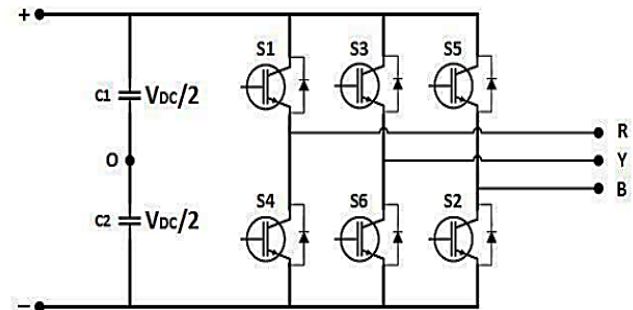


Figure 2. Variable frequency drive internal structure.
Source: M, Delgado, 2017

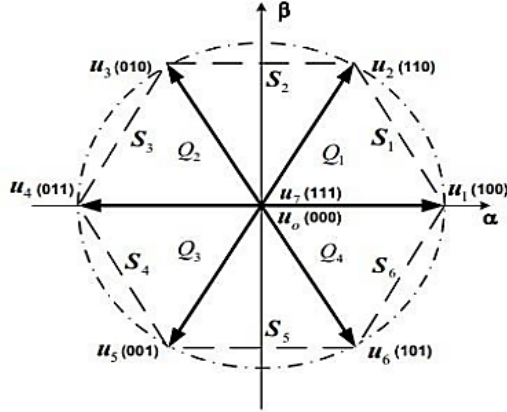


Figure 3. Regular hexagon, position of the switching states.
Source: M, Delgado, 2017

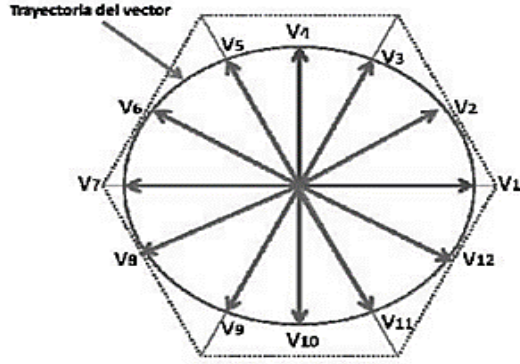


Figure 4. Complex plane with intermediate vectors.
Source: M, Delgado, 2017

In Fig. 4, the sectors are represented as S1, S2, S3, S4, S5, S6, the quadrants as Q1, Q2, Q3, Q4, the active vectors represent each edge and the 2 null vectors are in the center of the flat since they do not have a modulus value. These vectors are also called director vectors, they are the only ones that the 6-switch three-phase inverter can generate, therefore they are fixed in the complex plane, the more sinusoidal the output signal is and it directly produces fewer harmonics. [7]

The reference vector is the one that rotates throughout the plane presented above, it switches between the two director vectors depending on the sector in which it is located. [7]

2.3.2 Switching times

A The reference vector V_{ref} can be represented in the complex plane, but only with its closest direction vectors. According to this representation, the equations to determine the activation times of each vector are eq(1) eq(2) eq(3) eq(4):

$$T_1 = \frac{\sqrt{3}V_{ref} T_s}{V_{cc}} \sin\left(\frac{\pi}{3} - \alpha\right) \quad (1)$$

$$T_2 = \frac{\sqrt{3}V_{ref} T_s}{V_{cc}} \sin(\alpha) \quad (2)$$

$$T_0 = T_s - T_1 - T_2 \quad (3)$$

$$T_s = \frac{1}{6 * f} \quad (4)$$

Where:

T_s : Period in each sector

f : Frequency of the sinusoidal signal of the system, divide by 6 because there are 6 sectors

V_{ref} : Module of the reference vector

α : Angle between the reference vector and the direction vector

$V^* 1$ its values are between 0° and 60°

$\pi/3$: Angle between the two direction vectors, is equal to 60°

T_1 : Application time of the direction vector $V^* 1$

T_2 : Application time of the direction vector $V^* 2$

T_0 : Time of application of the null vector $V^* 0$ o $V^* 7$

2.3.2 Switching sequence

The activation time of the null vectors depends a lot on the distribution of the duty cycles, the use of two null vectors minimizes the content of harmonics in the signal but the switching losses increases, while with a single vector switching losses are minimized but harmonics increase, the switching sequences can be seen in table 1. [7]

With this, the shapes of the output signals in each sector would be those shown in Fig. 5:

Table 1

Vector sequence using 2 null vectors.

Zone	Sequence
1	V0-V1-V2-V7-V2-V1-V0
2	V0-V3-V2-V7-V2-V3-V0
3	V0-V3-V4-V7-V4-V3-V0
4	V0-V5-V4-V7-V4-V5-V0
5	V0-V5-V6-V7-V6-V5-V0
6	V0-V1-V6-V7-V6-V1-V0
7	V0-V1-V2-V7-V2-V1-V0
8	V0-V3-V2-V7-V2-V3-V0

Source: The author

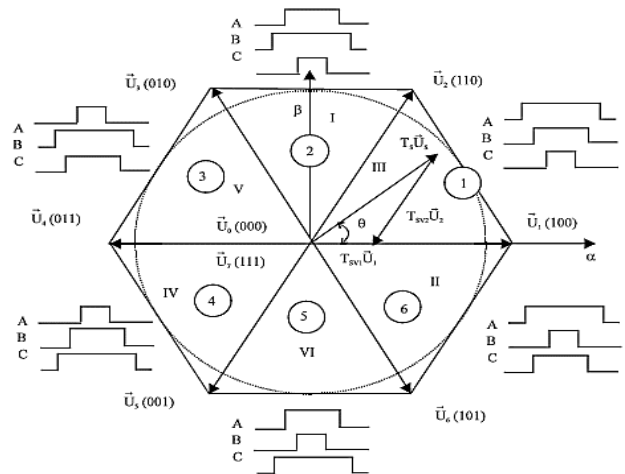


Figure 5. Full symmetrical alignment for all 6 sectors.

Source: M, Delgado, 2017

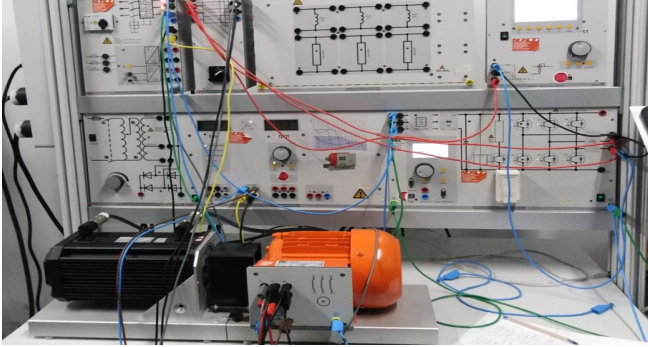


Figure 8. Training systems for electric machines, drivers and power electronics.
Source: The author.

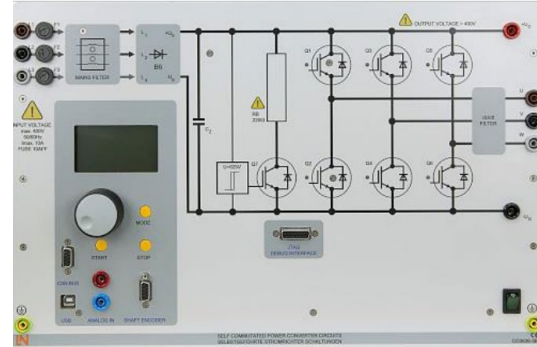


Figure 10. Forced Commutation Static Converters of Training systems for electric machines, drivers and power electronics.
Source: The author.



Figure 9. Source of Training systems for electric machines, drivers and power electronics
Source: The author.

- Outputs: o Three-phase current: L1, L2, L3, N through 4mm safety sockets
- Protection devices: o Motor protection circuit breaker, adjustable from 6.3A to 16A o Low voltage circuit breaker o Safety disconnect.
- Mains connection: 3 x 230/400V, 50/60Hz via CEE connector with 1.8m cable.

Fig. 10 shows the forced commutation static converters teaching system, which allows the assembly and analysis of power electronics circuits with IGBTs. In addition to power semiconductors, the system has activation and measurement devices for all variables. important.

- Control unit with 6-pulse IGBT inverter
- Activation and measurement unit controlled by means of digital signal processing
- Integrated measurement of 3 currents and 6 voltages
- Electronic control and disconnection due to overvoltage and overload
- Integrated control function for mounting controlled drives
- Interface for integration to the Matlab unit
- Selectable PWM frequencies
- USB port
- Input for incremental sensor
- Analog input
- Integrated brake chopper
- Connection voltage: 3 x 47 V at 220 V, 60 Hz
- Maximum output power: 1 kVA.

Fig. 11 shows the servomotor test bench is a complete system for the analysis of electrical machines and drives. It consists of a digital control unit, a brake and the ActiveServo software. The system combines the latest technology with easy handling.

The brake forms a self-cooling, asynchronous servo brake unit with resolver. The connection of the motor cable and the sensor is made by means of a plug-in connector proof against polarity reversal. The machine has thermal control and forms, with the control unit, a drift-free drive and brake system that does not need calibration.



Figure 11. Dynamic servo machine test system of Training systems for electric machines, drivers and power electronics
Source: The author.

- Maximum turning speed: 4000 rpm
- Maximum torque: 10 Nm
- Temperature monitoring: by means of a continuous sensor (KTY)
- Resolution of the resolver: 65536 pulses / revolution
- Dimensions: 275 x 210 x 210 mm (B x H x D).

Fig. 12 shows the image of the first machine used in the project, it has the following characteristics.

- Rated voltage: 400/230 V, 60 Hz
- Rated current: 0.95 A / 1.65 A
- Rated speed of rotation: 3600 rpm
- Rated power: 0.37 kW
- Cos phi: 0.76

Fig. 13 shows the image of the second machine used in the project, it has the following characteristics.

- Rated voltage: 400/230 V, 60 Hz
- Rated current: 3.8 A / 2.2 A
- Rated speed of rotation: 3600 rpm
- Rated power: 1 kW
- Cos phi: 0.83.

Fig. 14 shows the diagram connection of the system.



Figure 12. Three phase induction machine of Training systems for electric machines, drivers and power electronics.
Source: The author.



Figure 13. Three phase induction machine of Training systems for electric machines, drivers and power electronics.
Source: The author.

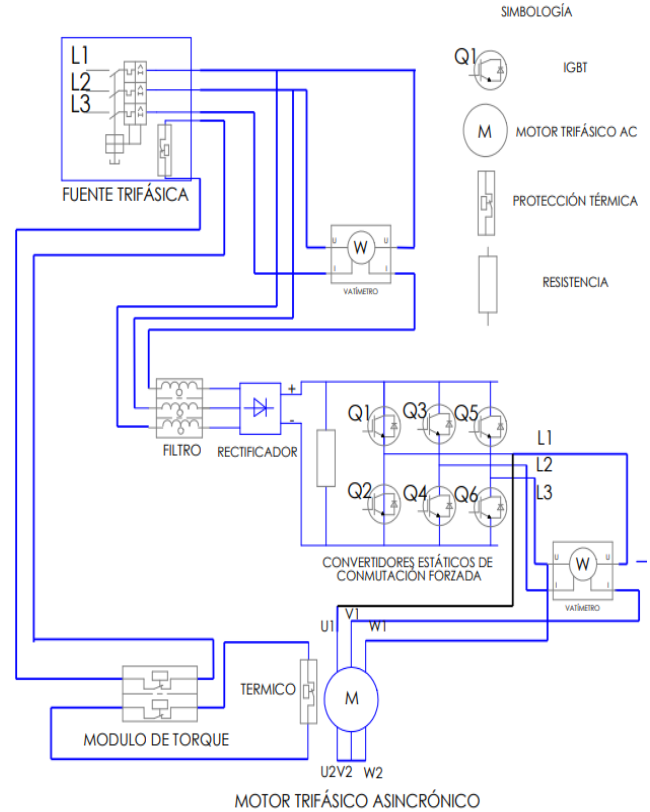


Figure 14. Physical system connection diagram.
Source: The author.

2. Methodology

To analyze the efficiency of the controller using the space vector pulse width modulation technique, the simulink library for control of a three-phase induction motor using SVPWM is used.

Subsequently, the parameterization of the electrical data of the equipment that is physically available in this case of the equipment of the "Training systems for electric machines, drivers and power electronics" created by the Lucas Nulle brand is carried out.

Next, three operating scenarios are considered at 200rpm at 1300rpm at 3600rpm, these three speeds operated with a load of 1.5 Nm, then power meters are implemented at the input and output of the controller dividing the output power for the power of input to obtain a value that is multiplied by 100%, additional semiconductor switching times are displayed.

Next, the physical system is implemented with the equipment of the "Training systems for electric machines, drivers and power electronics" according to the diagram in Fig. 16 where a wattmeter is connected to the input and output of the forced commutation static converter, then The torque module is configured to apply the load of 1.5Nm to monitor the system at speeds of 200rpm, 1300rpm and 3600rpm, a stabilization time of 1s is considered to take the values, avoiding starting values.

3. Results and analysis

An analysis of the SVPWM system is carried out to know the behavior and limits of operation, it is evaluated taking into account three speeds 200 rpm 1300rpm and 3600rpm maintaining a constant torque of $1.5N \cdot m$ in each case of speed parameter the efficiency of the controller is evaluated.

3.1 Case A 200rpm simulink.

Fig. 15 shows the input parameters to evaluate case A. The trigger signals for the semiconductor bridge in semiconductor Q1 changes state in the order of 248.641 ms, this signal can be seen in Figs. 16 and 17.

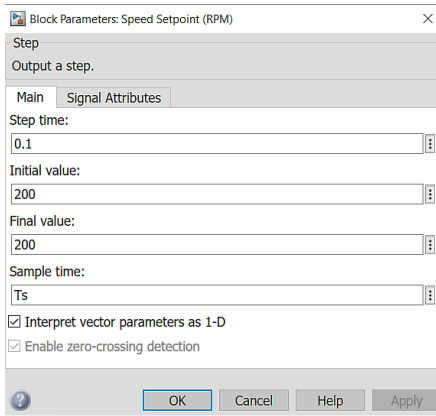


Figure 15. Data entry case A.
Source: The author.

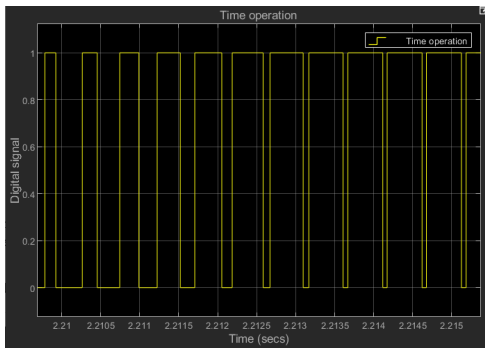


Figure 16. Semiconductor operating time case A.
Source: The author.

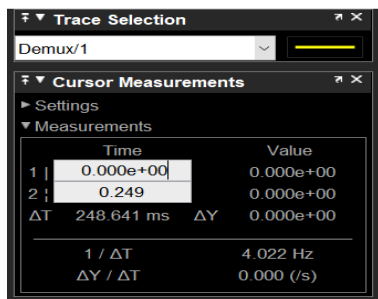


Figure 17. Semiconductor operating time case A.
Source: The author.

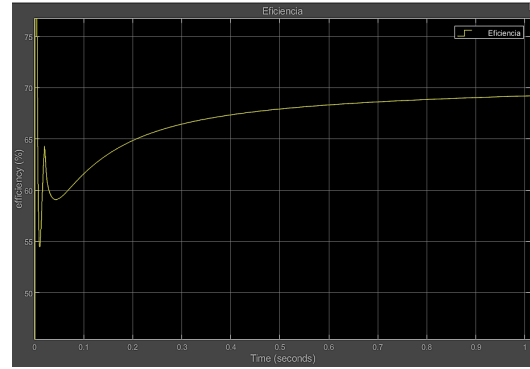


Figure 18. Inverter efficiency curve case A.
Source: The author.

Fig. 18 shows the behavior of the efficiency of the DC to AC voltage conversion stage. At the beginning of the curve, an unstable section is presented, this is due to the stabilization time of the system start-up, later it reaches an efficiency of 69%.

3.2 Case B 1300rpm simulink.

Fig. 19 shows the input parameters to evaluate case B. The trigger signals for the semiconductor bridge in semiconductor Q1 changes state in the order of 31.322 ms, this signal can be seen in Figs. 20 and 21.

Fig. 22 shows the behavior of the efficiency of the DC to AC voltage conversion stage. At the beginning of the curve, an unstable section is presented, this is due to the stabilization time of the system start-up, later it reaches an efficiency of 49%.

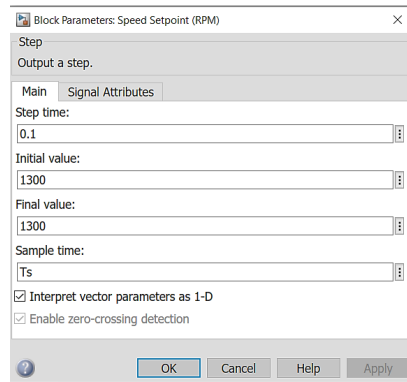


Figure 19. Data entry case A.
Source: The author.

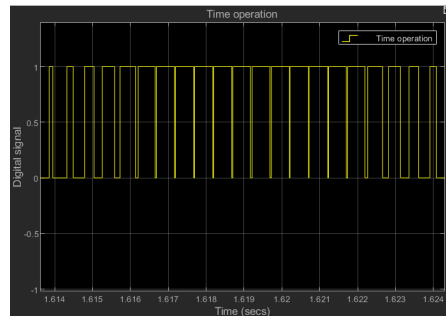


Figure 20. Semiconductor operating time case B.
Source: The author.

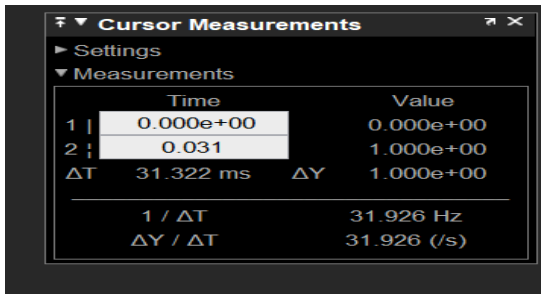


Figure 21. Semiconductor operating time case B.
Source: The author.

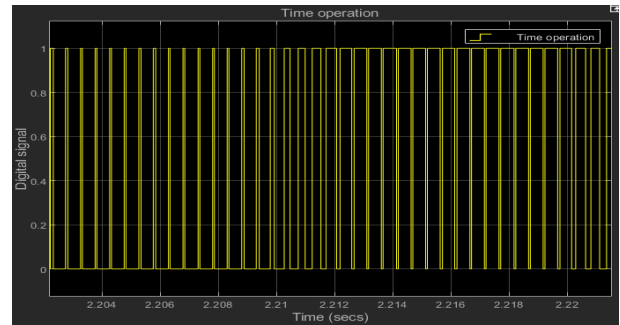


Figure 24. Semiconductor operating time case C.
Source: The author.

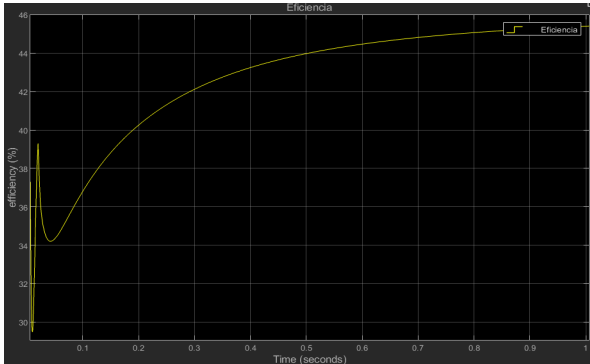


Figure 22. Inverter efficiency curve case A.
Source: The author.

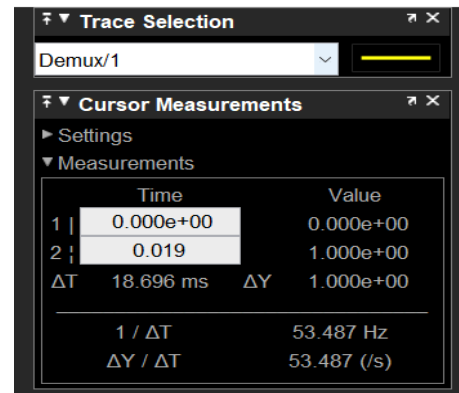


Figure 25. Semiconductor operating time case C.
Source: The author.

3.3 Case C 3600rpm simulink.

Block Parameters: Speed Setpoint (RPM)

Step

Output a step.

Main Signal Attributes

Step time: 0.1

Initial value: 3600

Final value: 3600

Sample time: Ts

☒ Interpret vector parameters as 1-D

☒ Enable zero-crossing detection

OK Cancel Help Apply

Figure 23. Data entry case C.
Source: The author.

Fig. 23 shows the input parameters to evaluate case C. The trigger signals for the semiconductor bridge in semiconductor Q1 changes state in the order of 16,696 ms, this signal can be seen in Figs. 24 and 25.

Fig. 26 shows the behavior of the efficiency of the DC to AC voltage conversion stage at the beginning of the curve, an unstable section is presented, this is due to the stabilization time of the system start-up, later it reaches an efficiency of 45.4%.

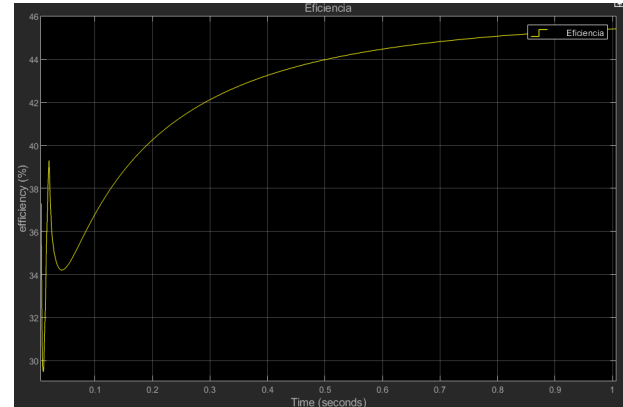


Figure 26. Inverter efficiency curve case C.
Source: The author.

3.4 Case A 200rpm in the training systems for electric machines, drivers and power electronics

In Fig. 27, in the first case, the torque input data is set at 1.5N*m and the speed at 200rpm.

With the data set in the first case, the results presented in Fig. 28 are obtained, a power of 72.6 VA at the output and a power of 99.9 VA at the input, generating an efficiency of 72.67%.



Figure 27. Data entry case A.
Source: The author.

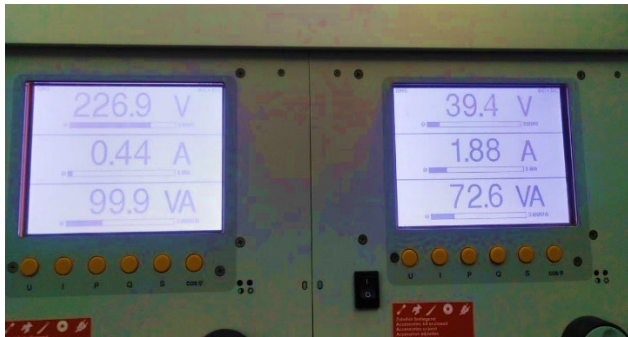


Figure 28. Power input and output measured data result.
Source: The author.

3.5 Case B 1300rpm in the Training systems for electric machines, drivers and power electronics

In Fig. 29, in the second case, the torque input data is set at 1.5N*m and the speed at 1300rpm.

With the data set, the results presented in Fig. 30 are obtained with a power of 165.4 VA at the output and a power of 336 VA at the input, generating an efficiency of 49.22%.



Figure 29. Data entry case B.
Source: The author.



Figure 30. Power input and output measured data result.
Source: The author.

3.6 Case C 3600rpm in the Training systems for electric machines, drivers and power electronics

In Fig. 31, in the second case, the torque input data is set at 1.5N*m and the speed at 3600rpm.

With the data set in the second case, the results presented in Fig. 32 are obtained, a power of 214.4 VA at the output and a power of 453 VA at the input, generating an efficiency of 47.32%.



Figure 31. Data entry case C.
Source: The author.



Figure 32. Power input and output measured data result.
Source: The author.

Table 2
Summary of cases physical system and mathematical model.

Cases	Speed (rpm)	Lucas Nulle Module (%)	Simulink mathematical model efficiency (%)	Error (%)
TO	200	72.67	69	5
B.	1300	49.22	49	0.4
C.	3600	47.32	45.4	4.05

Source: The author

Table 2 presents the summary of results comparing the physical system with the mathematical model, the minimum error reached is 0.4% and the maximum 5%.

The research is focused on the efficiency of the controller, subjecting the motors to different operating scenarios described in this section, the result of the efficiency of the controller varies because the efficiency of the controller depends on the switching speed of the IGBT's and this depends from the speed at which the motor rotates, for example, at a motor speed of 200 rpm, the switching speed of the IGBTs is 248.641 ms and the efficiency of the controller is 69%.

Next, the signals of the induction motor will be studied, focusing on the torque to define the operating limits of the controller, maintaining a desired torque signal.

3.7 Electric motor parameter result

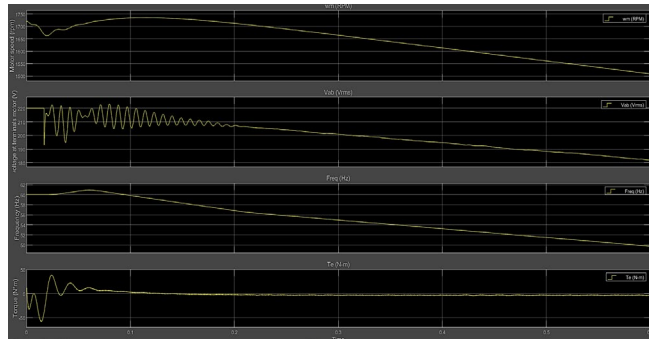


Figure 33. Electric motor parameter result 500rpm.
Source: The author.

Fig. 33 shows the speed and torque parameters of the motor at 500rpm, we can see that the torque remains constant.

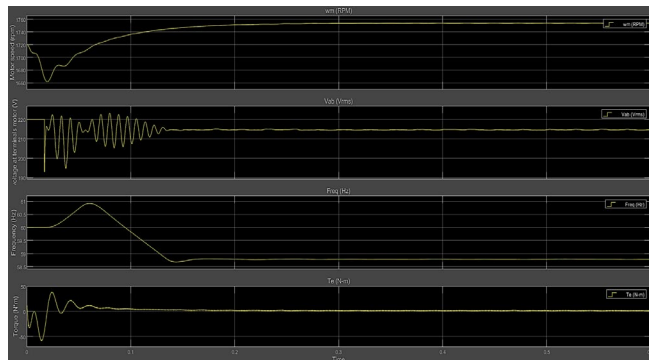


Figure 34 Electric motor parameter result 1700rpm.
Source: The author.

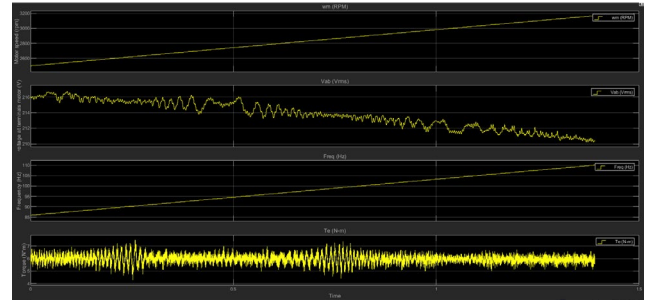


Figure 35 Electric motor parameter result 3600rpm.
Source: The author.

Fig. 34 shows the speed and torque parameters of the motor at 1700rpm, we can see that the torque signal remains constant.

Fig. 35 shows the speed and torque parameters of the motor at 3600rpm, we can see that the torque signal loses the desired value.

It is also observed through laboratory tests that operating the engine at a speed below 500rpm tends to stall and lose torque. Because the engine presents an error of 5% running at 200rpm and 4.05% running at 3600rpm, it is decided to define the ideal operating ranges between 500rpm and 1700rpm.

4. Conclusions

Analyzing the system in direct interaction with the engine's operating parameters, the speed range in which the tests were carried out was from 200rpm to 3600rpm, however, after evidencing an irregular behavior in torque maintenance under load conditions, a stable operating range between 500rpm to 1725rpm because the engine torque remains constant within this operating range, outside these limits we have an increase in the error that is presented in table 2 and this compromises the desired torque control.

Operating the system below 500 rpm, the error of the system compared to the validation with the physical system reaches a value of 5% and also another important problem that occurs in the physical system at speeds below 500rpm tends to lose the magnetization that results in a standstill of the motor having an output torque of zero newtons per meter, on the other hand at speeds greater than 1725 rpm the system requires a switching speed close to 18.696ms in the semiconductor block, and the torque of the machine no longer it remains constant as can be seen in Exhibit 2 with a speed of 3600 rpm.

The efficiency of the system at a speed of 1725 rpm reaches values close to 45% and the error compared to the physical system reaches a value of 4%, for this reason the mathematical model could no longer be trusted outside this limit.

References

- [1] González-Tamayo, J.P., y Avendaño-González, L.E., Simulación de control vectorial a un motor de inducción. Scientia Et Technica, 18(1), pp. 1-10, 2013. DOI: <https://doi.org/10.22517/23447214.7115>

- [2] Dalvand, H. and Zare, M., Techno-economic evaluation of energy efficiency measures in iranian industrial 3-phase electric motors, in: First Int. Power Energy Conf. (PECon 2006). Proc., 2006, pp. 1-5. DOI: <https://doi.org/10.1109/PECON.2006.346608>.
- [3] ABB, El gasto energético en la industria | ABB, [en línea]. 2018. [consultado: Feb. 02, 2023]. Disponible en: <https://new.abb.com/drives/es/eficiencia-energetica/gasto-energetico-industria>
- [4] Kun, W., Xiaojie, Y., Chenchen, W. and Minglei, Z., An equivalent dual three-phase SVPWM realization of the modified 24-sector SVPWM strategy for asymmetrical dual stator induction machine, ECCE 2016 - IEEE Energy Convers. Congr. Expo. Proc., no. 51507009, 2016, DOI: <https://doi.org/10.1109/ECCE.2016.7854842>.
- [5] Sánchez-Gamboa, F.I., Análisis de la eficiencia del control de un motor asincrónico mediante SVPWM en lazo abierto, Tesis, Universidad Técnica de Cotopaxi, Ecuador, 2022.
- [6] González, J.D., Inversores Pwm, 2018, pp. 1-26. [Online]. Available at: <http://ieec-pels-ics.es/Pels/Pdf/LeccionInversoresJuanDiaz.pdf>.
- [7] Delgado, M.Á.A., Desarrollo de un módulo SVPWM con un controlador en lazo cerrado para la Universidad Politécnica Salesiana, 2013.

F.I. Sanchez-Gamboa, received the BSc. Eng. in Electromechanical Engineering in 2016, from the University of the Armed Forces ESPE of Latacunga. Cotopaxi, Ecuador. From 2009 to 2016, received MSc. in Electromechanical Engineering in 2022, from the Cotopaxi Technical University, he worked as a transformer design engineer for electricity companies within the power sector and since 2019 for the Instituto Superior Tecnológico Cotopaxi. Currently, he is a full professor in the Electromechanical department and research Department, Instituto Superior Tecnológico Cotopaxi. His research interests include: design, modeling of drivers and electric motors.
ORCID: 0000-0001-8390-6200